

See discussions, stats, and author profiles for this publication at: <https://www.researchgate.net/publication/26874163>

Localization of Na⁺-K⁺ ATPases in Quasi-Native Cell Membranes

ARTICLE in NANO LETTERS · OCTOBER 2009

Impact Factor: 13.59 · DOI: 10.1021/nl902803m · Source: PubMed

CITATIONS

30

READS

35

7 AUTHORS, INCLUDING:



Janguang Jiang

Chinese Academy of Sciences

109 PUBLICATIONS 1,504 CITATIONS

SEE PROFILE



Mingjun Cai

27 PUBLICATIONS 240 CITATIONS

SEE PROFILE



Yuping Shan

Chinese Academy of Sciences

25 PUBLICATIONS 232 CITATIONS

SEE PROFILE



Zhiyong Tang

National Center for Nanoscience and Tech...

200 PUBLICATIONS 9,571 CITATIONS

SEE PROFILE

Localization of $\text{Na}^+ - \text{K}^+$ ATPases in Quasi-Native Cell Membranes

Junguang Jiang,^{†,||} Xian Hao,^{†,‡,||} Mingjun Cai,[†] Yuping Shan,^{†,‡} Xin Shang,[†]
Zhiyong Tang,[§] and Hongda Wang^{*,†}

State Key Laboratory of Electroanalytical Chemistry, Changchun Institute of Applied Chemistry, Chinese Academy of Sciences, Changchun, Jilin 130022, People's Republic of China, Graduate School of Chinese Academy of Sciences, Beijing 100049, and People's Republic of China, National Center for Nanoscience and Technology, Beijing 100190, People's Republic of China

Received August 27, 2009; Revised Manuscript Received September 22, 2009

ABSTRACT

$\text{Na}^+ - \text{K}^+$ ATPases have been observed and located by in situ AFM and single molecule recognition technique, topography and recognition imaging (TREC) that is a unique technique to specifically identify single protein in complex during AFM imaging. $\text{Na}^+ - \text{K}^+$ ATPases were well distributed in the inner leaflet of cell membranes with about 10% aggregations in total recognized proteins. The height of $\text{Na}^+ - \text{K}^+$ ATPases measured by AFM is in the range of 12–14 nm, which is very consistent with the cryoelectron microscopy result. The unbinding force between $\text{Na}^+ - \text{K}^+$ ATPases in the membrane and anti-ATPases on the AFM tip is about 80 pN with the apparent loading rate at 40 nN/s. Our results show the first visualization of an essential membrane protein, $\text{Na}^+ - \text{K}^+$ ATPase, in quasi-native cell membranes and may be significant to reveal the interactions between $\text{Na}^+ - \text{K}^+$ ATPases and other membrane proteins at the molecular level.

$\text{Na}^+ - \text{K}^+$ ATPase, a key transmembrane protein, utilizes energy from ATP hydrolysis to balance the concentration of Na^+ and K^+ across cell membranes.¹ The structure and function of $\text{Na}^+ - \text{K}^+$ ATPase have been intensely studied since its original description in 1957.² More excitingly, the fine crystal structure of $\text{Na}^+ - \text{K}^+$ ATPase was successfully reported a year ago despite the difficulty of sample preparation for X-ray analysis.³ The following important questions about the $\text{Na}^+ - \text{K}^+$ ATPase could be to explore the location of $\text{Na}^+ - \text{K}^+$ ATPases in cell membranes and the relationship between $\text{Na}^+ - \text{K}^+$ ATPases and other membrane proteins due to their importance for understanding single molecule mechanism in living cells. However, to date, the morphology and location of $\text{Na}^+ - \text{K}^+$ ATPases in native cell membranes is still an unclear topic.

There has been much progress in using fluorescent microscopy for the localization of single molecule in complex system, but its low spatial resolution made it difficult to locate proteins at a few nanometers resolution.⁴ Atomic force microscope (AFM) has been a powerful tool to observe molecular interactions due to its high resolution and ability to image in variable environments.^{5–7} Recently, TREC has

been developed to expand AFM's application for recognizing specific single molecule such as chromatin or protein complex.^{8–12} TREC scans a sample with a functionalized AFM tip (e.g., antibody-tethered tip). A topographic image is generated simultaneously and in exact spatial registration with a recognition image that locates the sites of specifically binding events (e.g., antigen–antibody recognition), leading to accurately position the specific individual molecules within the topographic image. The recognition process between a tip-tethered molecule and its recognition counterpart on surface is highly efficient and specific. TREC has been successfully used in the single and small molecule recognition. However, mapping more sophisticated native system at molecular resolution, such as unfixed live cells and cell membranes, is still a significant interest for the TREC's application.^{13–15} Herein, we applied TREC to localize ATPases in quasi-native cell membranes under physiological conditions.

Human red blood cells (hRBC) were used due to their simplification and their capacity of abundant $\text{Na}^+ - \text{K}^+$ ATPases.¹ hRBC were immobilized on APTES-mica and sheared open by low salt PBS buffer without any fixation.¹⁶ This method provides the cell membranes in their near-native state. There may be two types of forces involved to break the hRBC by the low salt buffer. One is the hypotonic force to open the hRBC from the inside of the cells, and the other one is the shear force that could break the RBC membrane

* To whom correspondence should be addressed. E-mail: hdwang@ciac.jl.cn.

[†] Changchun Institute of Applied Chemistry, Chinese Academy of Sciences.

[‡] Graduate School of Chinese Academy of Sciences.

[§] National Center for Nanoscience and Technology.

^{||} These authors contributed equally to this paper.

from the outside of the cells. The transmembrane proteins were expected to be kept well due to their insertion in the lipid bilayers. The membrane skeletons were easily washed away by the low salt buffer¹⁶ so that we obtained the clean cell membranes by the single-step preparation. However, this method is not suitable for the skeleton study of cell membranes because the skeleton was destroyed by the stream of low salt buffer.

We selected mica as substrate because of its atomic flat surface that has minimum effect on the feature of cell membranes. There are abundant amino-groups on the APTES-mica surface so that hRBC membranes were attached onto the surface tightly. We also tried to use the mica and glass surface without APTES modification; however, the hRBC membranes were not attached onto the substrate stably.

Figure 1A shows the dense inside-out membrane patches of hRBC. The cell membranes were well distributed on the surface. The inner leaflet of cell membranes is upward oriented for AFM imaging as the outer leaflet of cell membranes has been attached onto the APTES-mica tightly, and the whole blood cell has been opened.¹⁶ The width of the cell membranes is about 6–8 μm , which indicates that the bottom layer of hRBC was well attached onto the APTES-mica. To verify the existence of $\text{Na}^+ - \text{K}^+$ ATPases in the inner leaflet of cell membranes, we observed the cell membranes with QDs (quantum dots) functionalized anti-ATPase by fluorescence microscopy. Figure 1B shows the patches of cell membranes (green), which indicate that there are abundant $\text{Na}^+ - \text{K}^+$ ATPases in the inner leaflet of cell membranes. The control experiment with only QDs (Figure 1C) shows very low signal due to the lack of anti-ATPase. We also incubated the unrelated protein (MNA-M lectin with QDs) as control experiment, which showed there was no fluorescence signal from membrane patches observed.

To reveal more detailed structure and locate the $\text{Na}^+ - \text{K}^+$ ATPases in the inner leaflet of cell membranes, we image the membrane patches by anti-ATPase-functionalized AFM tip. Figure 2 illustrates the feature of TREC. The AFM tip was functionalized with an antibody by a heterobifunctional PEG linker as shown in Figure 2A. The antibody on the tip is flexible, which is very suitable for the antibody–antigen recognition. With the tip scanning the complex sample (Figure 2B), the antibody would specifically bind to the corresponding antigen, which induces the recognition signal.

Figure 3A shows the typical image of inside-out cell membranes in which the particles that are supposed to be membrane proteins are clearly observed. The proteins display a broad height distribution between 3 and 14 nm with the multiple peaks (Figure 3Q), which indicates that there are multiple types of proteins in the inner leaflet of cell membranes. Figure 3C–F shows the magnification of membrane proteins in which proteins with different size are observed next to each other. In order to identify ATPases, we acquired the recognition image by TREC mode simultaneously. The Figure 3B shows the corresponding recognition image by anti-ATPase-functionalized AFM tip. The dark spots represent the proteins recognized by the anti-ATPases. Figure 3G–J shows the magnified recognition image corresponding

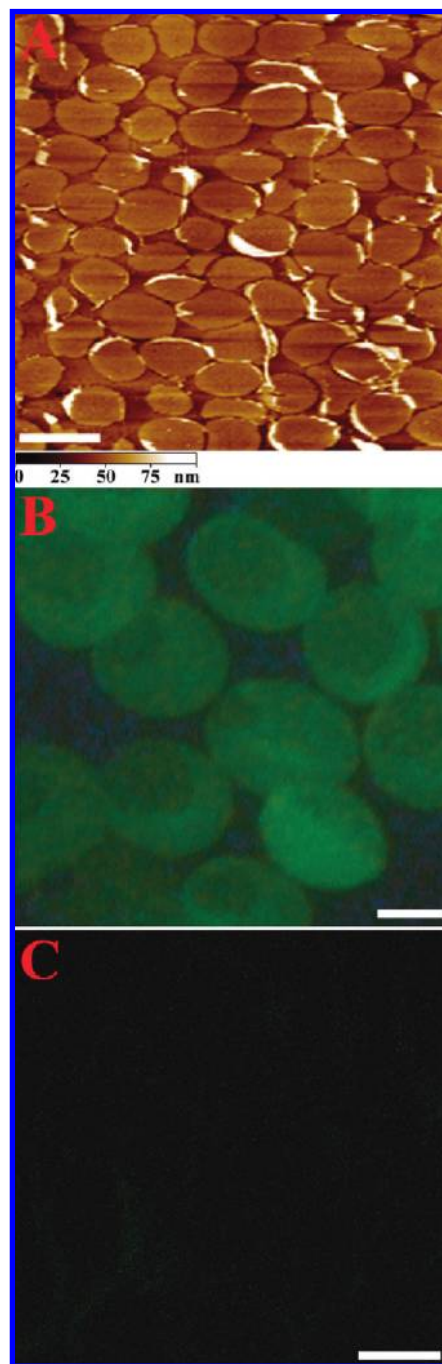


Figure 1. (A) AFM image of inside-out hRBC membranes. Scale bar is 15 μm . (B) Inside-out hRBC membranes (green patches) labeled with anti-ATPase-QDs. The scale bar is 4 μm . (C) Control experiment, the membranes were treated by QDs without anti-ATPase. The signal from nonspecific interaction and background is very low. The scale bar is 6 μm .

to Figure 3C–F, respectively. To verify the specific recognition signal, we repetitively scanned the same location. The recognition signal was almost located at the same sites, which indicates the dark signal was from the interactions between anti-ATPases on AFM tip and $\text{Na}^+ - \text{K}^+$ ATPases in the membrane but not from noise. To test the specificity of the recognition signal, we flew the blocking reagent (free anti-ATPase) into the liquid cell during imaging. The recognition signal was abolished after 10 min (Figure 3K). Thus, the

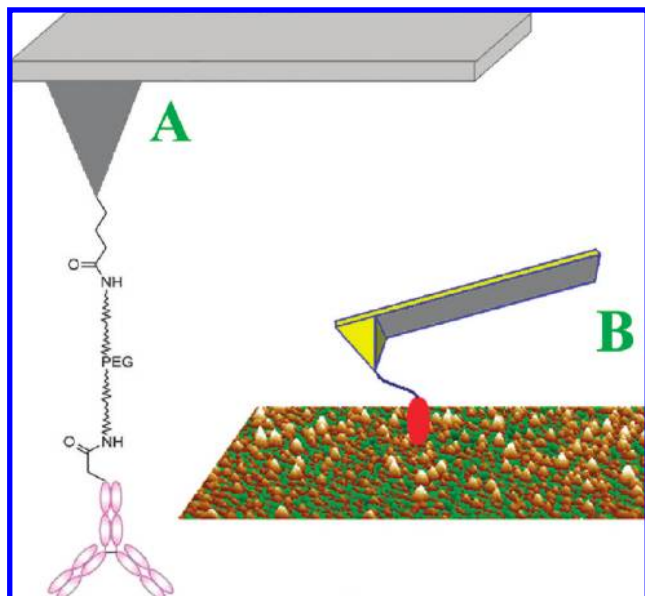


Figure 2. Illustration of antibody-functionalized AFM tip. (A) The AFM tip functionalized with an antibody by a heterobifunctional PEG linker. (B) The antibody-attached AFM tip scans the complex sample. The antibody would temporally bind the antigen on the surface during scanning.

ability of the tip-tethered anti-ATPase to produce a recognition signal (Figure 3B) was specifically blocked by an excess of free anti-ATPases in solution, demonstrating that the recognition signals came from interactions between the anti-ATPases on the tip and Na^+/K^+ ATPases in the inner membrane. Figure 3M shows a magnifying recognition site with cross section analysis shown in Figure 3N. The amplitude reduction of AFM cantilever caused by recognition events (recognition signal) was about 2.2 nm (Figure 3N). Figure 3O shows one blocked area corresponding to Figure 3M. The cross section analysis (Figure 3P) indicates that the recognition signal was blocked efficiently (<0.7 nm). We tried to observe Na^+/K^+ ATPases at high resolution; however, no further detail was obtained. We assumed that the proteins were irregularly distributed in the inner membrane, therefore it was much difficult for AFM to obtain high resolution image like a crystalline protein array.¹⁷

To clarify the distribution of Na^+/K^+ ATPases in the membrane, we marked the recognition signal by green dots, and superimposed the recognition signal onto the topographic image (Figure 3L). We noticed the recognition signal was mainly on the proteins with the height of about 12–14 nm, which might be a little lower than the actual height of Na^+/K^+ ATPase due to the AFM tip pressure. This result is supported by the cryoelectron microscopy result in which the average height of ATPases was calculated at about 15 nm.¹⁸ In addition, Na^+/K^+ ATPases appeared to be well distributed in the membrane with only about 10% aggregations marked by the blue arrows in Figure 3B, which may be related to the associated proteins of Na^+/K^+ ATPases.

To further test the specific interaction between the Na^+/K^+ ATPases in the membrane and the anti-ATPases on the AFM tip, we did the force curve measurement in the inner leaflet of cell membranes. The inset A in Figure 4

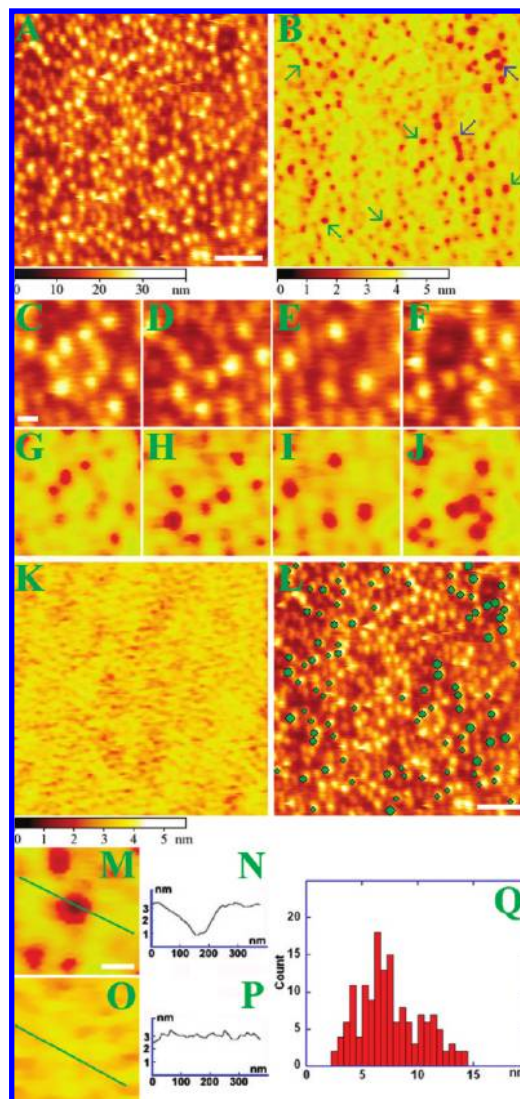


Figure 3. (A) Topographic image of the inner leaflet of cell membranes. Scale bar is 500 nm. (B) Corresponding recognition image of Na^+/K^+ ATPases (dark spots). Red and blue arrows indicate isolated Na^+/K^+ ATPases and Na^+/K^+ ATPase aggregations, representively. (C–F) Magnified topographic image of the inner membrane. Scale bar is 100 nm. (G–J) Magnified recognition image corresponding to figure 3C–F. (K) Recognition image of Na^+/K^+ ATPases after blocking by free anti-ATPases. (L) Topographic image of the inner cell membrane with recognition spots superimposed by overlaying them (green dots) on the top of the topographic images. Scale bar is 500 nm. (M) Magnifying recognition image from Figure 3B. Scale bar is 100 nm. (N) Cross section analysis along the line in Figure 3M. (O) Magnifying recognition image from Figure 3K. (P) Cross section analysis along the line in Figure 3O. (Q) The height distribution of proteins in the inner leaflet of cell membranes.

shows a typical unbinding event. The stretch length of the force curve (about 50 nm) is larger than the length of the cross-linker PEG (about 20 nm) because it includes the stretch length of PEG linker and the bending displacement of the cantilever.¹⁹ The histogram includes 250 unbinding force curves. The major peak is about 80 pN with the apparent loading rate (cantilever spring constant multiplied by retraction velocity²⁰) at 40 nN/s, which is in the range of antibody and antigen unbinding force and much larger than

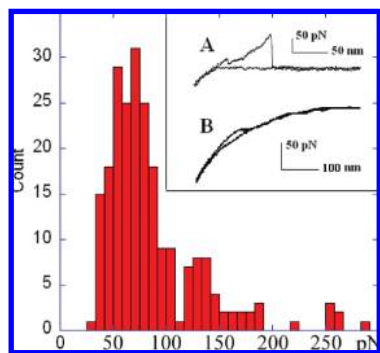


Figure 4. Distribution of unbinding force between the $\text{Na}^+ - \text{K}^+$ ATPases in the inner leaflet of cell membranes and the anti-ATPases on the AFM tip. A typical approach and retraction curve is shown as the inset A. A typical force curve after blocking by free ATPases is shown as the inset B.

nonspecific force (less than 20 pN).⁹ The insert B in Figure 4 shows the typical force curve without unbinding peak after blocking by free ATPases, which is consistent with the recognition image in Figure 2.

In summary, we have first observed and located $\text{Na}^+ - \text{K}^+$ ATPases in quasi-native cell membranes by in situ AFM and TREC. $\text{Na}^+ - \text{K}^+$ ATPases in the inner membrane appear to be a type of large protein with the height of 12–14 nm. $\text{Na}^+ - \text{K}^+$ ATPases are distributed well in the membrane with few aggregations. The unbinding force between $\text{Na}^+ - \text{K}^+$ ATPases in the membrane and anti-ATPases on the tip is about 80 pN with the apparent loading rate at 40 nN/s. Our results may be significant to reveal the hierarchy of cell membranes and pave the way for exciting opportunities in mapping transmembrane proteins and exploring the interactions among membrane proteins at single molecular level.

Experimental Section. APTES Functionalized Mica. A desiccator was purged with argon for 2 min, and 30 μL of APTES (aminopropyltriethoxysilane, 99%, Sigma-Aldrich, St. Louis, MO) was placed into a small container at the bottom of the desiccator.²¹ Ten microliters of *N,N*-diisopropylethylamine (99%, distilled, Sigma-Aldrich) was placed into another small container, and the desiccator purged with argon for a further 2 min. Mica sheets were stripped on one side until smooth and immediately placed into the desiccator. The desiccator was purged for another 3 min and then sealed off, leaving the mica exposed to APTES vapor for 1 h. After this exposure, the APTES was removed, the desiccator was purged, and the treated mica (AP-mica) was stored in the sealed desiccator until needed.

Preparing Cell Membranes. To prepare hRBC, two drops of fresh human blood from healthy donor (B-type) were washed five times in 150 mM PBS buffer (pH 7.5). The diluted hRBC were deposited onto AP-mica for 15 min. To obtain the inner membrane without membrane skeleton proteins in one-step preparation, hRBC attached to APTES-mica were sheared open by a fast stream of 7.5 mM PBS (pH 7.5) through a needle at an angle of 20° .¹⁶ Cell membranes were imaged in the PBS buffer (pH 7.5) after preparation immediately.

AFM Recognition Imaging. Silicon-nitride cantilever tips with a spring constant of 0.1 N/m (Microlever, Veeco, Santa

Barbara, CA, coated for MacMode AFM by Agilent Technologies, Chandler, AZ) for recognition imaging were modified as described.⁹ Monoclonal antibody to pan alpha sodium–potassium ATPases that binds all alpha subunits in human, sheep, dog, pig, and chicken were obtained from Abcam (Catalog number ab2871). $\text{Na}^+ - \text{K}^+$ ATPase antibody was reacted with *N*-succinimidyl 3-(acetylthio) propionate (SATP, Sigma inc.) and purified in a PD-10 column (Amersham Pharmacia Biotech). The cantilevers were cleaned in a UV cleaner, vapor treated with APTES, and reacted with PEG cross-linker (molecular weight = 2000 Da, JenKem Technology Co., Ltd., Beijing) using triethylamine and CHCl_3 . The SATP-labeled antibodies were then bound to the PEG cross-linkers with NH_2OH (Sigma) in NaCl/Phosphate buffer. The tips were then rinsed in PBS buffer (pH 7.5) and stored at 4°C until use. Imaging was acquired on a 5500 AFM with a PicoTREC recognition imaging attachment (Agilent Technologies, Chandler AZ). Recognition images were captured as 512×512 pixels images at 70% set point and scan rates of 1 Hz. Recognition blocking experiment was done by flowing through 100 μL 25 $\mu\text{g}/\text{mL}$ ATPase solution (in PBS, pH 7.5) into AFM liquid cell.

Data Analysis. The heights and widths of membrane proteins were measured using PicoScan 5.3.3 software (Agilent Technologies, Chandler AZ). A maximum height was taken as the peak height relative to the local background. Recognition imaging was analyzed by a software, Recognition Imaging Analysis.^{22,23} This program compiles histograms of the pixel intensity distribution from background regions containing no features and compares them to regions containing visible recognition spots. Recognition events give rise to a second peak in the intensity distribution and these were clearly separated from the background by selecting a cutoff of 75% of the background intensity (recognition spots correspond to a decrease in the signal).

Fluorescence Image. The mercaptopropionic acid (MPA) capped CdTe nanoparticles were prepared by following the recipe reported in the literature.²⁴ The prepared CdTe nanoparticles have a maximum photoluminescence peak at 540 nm and average diameters of 2.5 nm. Conjugation of MPA-CdTe with Anti-ATPase was prepared as follows: 10 μL of 1-ethyl-3-(3-dimethylaminopropyl) carbodiimide hydrochloride (EDAC) (10 mM) solution and 10 μL of *N*-hydroxysuccinimide (NHS) (10 mM) solution were added to 100 μL of MPA-capped CdTe (2.98 μm) PBS buffer solution. Then an appropriate amount of anti-ATPase was added to the reaction mixture. The reaction solution was incubated at room temperature overnight with continuous gentle stirring. The Anti-ATPase-CdTe conjugate was purified through a 100k molecular weight cutoff (MWCO) Microcon centrifugal filter device (Millipore, Inc.), and stored at 4°C .

To obtain the inner leaflet of cell membranes, hRBC attached to APTES-mica were sheared open by a fast stream of 7.5 mM PBS as described.¹⁶ Five microliters of Anti-ATPase-CdTe conjugate solution was added onto the inner membrane for 1 h and washed with PBS buffer 4 times before imaging. Cell membranes were imaged in the 150

mM PBS buffer (pH 7.5) on a Nikon EclipseTi Series microscope.

Acknowledgment. This work was supported by National Natural Science Foundation of China (NSFC, Grants 20735003 and 20975098).

References

- (1) Raess, B. U.; Tunnichliff, G. The Humana Press Inc.: 1989.
- (2) Skou, J. C. *Biochim. Biophys. Acta* **1957**, *1000*, 439–446.
- (3) Morth, J. P.; Pedersen, B. P.; Toustrup-Jensen, M. S.; Sorensen, T. L. M.; Petersen, J.; Andersen, J. P.; Vilsen, B.; Nissen, P. *Nature* **2007**, *450* (7172), 1043–U6.
- (4) Schutz, G. J.; Kada, G.; Pastushenko, V. P.; Schindler, H. *EMBO J.* **2000**, *19* (5), 892–901.
- (5) Han, W. H.; Lindsay, S. M.; Dlakic, M.; Harrington, R. E. *Nature* **1997**, *386* (6625), 563–563.
- (6) Peng, Q.; Li, H. B. *Proc. Natl. Acad. Sci. U.S.A.* **2008**, *105* (6), 1885–1890.
- (7) Schillers, H. *Pfluegers Arch.* **2008**, *456* (1), 163–177.
- (8) Stroh, C. M.; Ebner, A.; Geretschlager, M.; Freudenthaler, G.; Kienberger, F.; Kamruzzahan, A. S. M.; Smith-Gil, S. J.; Gruber, H. J.; Hinterdorfer, P. *Biophys. J.* **2004**, *87* (3), 1981–1990.
- (9) Stroh, C.; Wang, H.; Bash, R.; Ashcroft, B.; Nelson, J.; Gruber, H.; Lohr, D.; Lindsay, S. M.; Hinterdorfer, P. *Proc. Natl. Acad. Sci. U.S.A.* **2004**, *101* (34), 12503–12507.
- (10) Hinterdorfer, P.; Dufrene, Y. F. *Nat. Methods* **2006**, *3* (5), 347–355.
- (11) Wang, H.; Bash, R.; Lohr, D. *Anal. Biochem.* **2007**, *361* (2), 273–279.
- (12) Wang, H. D.; Obenauer–Kutner, L.; Lin, M.; Huang, Y. P.; Grace, M. J.; Lindsay, S. M. *J. Am. Chem. Soc.* **2008**, *130* (26), 8154–8155.
- (13) Chitchevlova, L. A.; Atalar, F.; Ozbek, U.; Wildling, L.; Ebner, A.; Hinterdorfer, P. *Pfluegers Arch.* **2008**, *456* (1), 247–254.
- (14) Ebner, A.; Nikova, D.; Lange, T.; Haberle, J.; Falk, S.; Dubbers, A.; Bruns, R.; Hinterdorfer, P.; Oberleithner, H.; Schillers, H. *Nanotechnology* **2008**, *19*, (38).
- (15) Lee, S.; Mandic, J.; Van Vliet, K. J. *Proc. Natl. Acad. Sci. U.S.A.* **2007**, *104* (23), 9609–9614.
- (16) Lange, T.; Jungmann, P.; Haberle, J.; Falk, S.; Duebbers, A.; Bruns, R.; Ebner, A.; Hinterdorfer, P.; Oberleithner, H.; Schillers, H. *Mol. Membr. Biol.* **2006**, *23* (4), 317–323.
- (17) Tang, J. L.; Ebner, A.; Badelt-Lichtblau, H.; Vollenkle, C.; Rankl, C.; Kraxberger, B.; Leitner, M.; Wildling, L.; Gruber, H. J.; Sleytr, U. B.; Ilk, N.; Hinterdorfer, P. *Nano Lett.* **2008**, *8* (12), 4312–4319.
- (18) Hebert, H.; Purhonen, P.; Vorum, H.; Thomsen, K.; Maunsbach, A. B. *J. Mol. Biol.* **2001**, *314* (3), 479–494.
- (19) Arrondo, J.; Alonso, A. Springer-Verlag: Berlin Heidelberg, 2006; p 177.
- (20) Krasnoslobodtsev, A. V.; Shlyakhtenko, L. S.; Lyubchenko, Y. L. *J. Mol. Biol.* **2007**, *365* (5), 1407–1416.
- (21) Lyubchenko, Y.; Shlyakhtenko, L.; Harrington, R.; Oden, P.; Lindsay, S. *Proc. Natl. Acad. Sci. U.S.A.* **1993**, *90* (6), 2137–2140.
- (22) Lin, L.; Wang, H. D.; Liu, Y.; Yan, H.; Lindsay, S. *Biophys. J.* **2006**, *90* (11), 4236–4238.
- (23) Wang, H.; Dalal, Y.; Henikoff, S.; Lindsay, S. *Epigenet. Chromatin* **2008**, *1*, 10.
- (24) Gaponik, N.; Talapin, D. V.; Rogach, A. L.; Hoppe, K.; Shevchenko, E. V.; Kornowski, A.; Eychmuller, A.; Weller, H. *J. Phys. Chem. B* **2002**, *106* (29), 7177–7185.

NL902803M